Phase-sensitive amplification of light in a $\chi^{(3)}$ photonic chip using a dispersion engineered chalcogenide ridge waveguide

Richard Neo,[1] Jochen Schröder,[1*] Yvan Paquot,[1] Duk-Yong Choi,[2] Steve Madden,[2] Barry Luther-Davies,[2] and Benjamin J. Eggleton[1]

[1]*Centre for Ultrahigh bandwidth Devices for Optical Systems (CUDOS), Institute of Photonics and Optical Science (IPOS) School of Physics, University of Sydney, NSW 2006, Australia*

[2]*CUDOS, Laser Physics Centre, Research School of Physics and Engineering, Australian National University, Canberra, ACT 0200, Australia*

[*]*jochen.schroeder@sydney.edu.au*

Abstract: We report phase-sensitive amplification of light using $\chi^{(3)}$ parametric processes in a chalcogenide ridge waveguide. By spectrally slicing pump, signal and idler waves from a single pulsed source, we are able to observe 9.9 dB of on-chip phase-sensitive extinction with a signal-degenerate dual pump four-wave mixing architecture in good agreement with numerical simulations.

OCIS codes: (190.4380) Nonlinear optics, four-wave mixing; (190.4410) Nonlinear optics, parametric processes.

References and links

1. C. Lundström, Z. Tong, M. Karlsson, and P. A. Andrekson, "Phase-to-phase and phase-to-amplitude transfer characteristics of a nondegenerate-idler phase-sensitive amplifier," Opt. Lett. **36**(22), 4356–4358 (2011).
2. C. Lundström, B. Corcoran, M. Karlsson, and P. A. Andrekson, "Phase and amplitude characteristics of a phase-sensitive amplifier operating in gain saturation," Opt. Express **20**(19), 21400–21412 (2012).
3. R. Slavik, F. Parmigiani, J. Kakande, C. Lundström, M. Sjödin, P. A. Andrekson, R. Weerasuriya, S. Sygletos, A. D. Ellis, L. Grüner-Nielsen, D. Jakobsen, S. Herstrm, R. Phelan, J. O'Gorman, A. Bogris, D. Syvridis, S. Dasgupta, P. Petropoulos, and D. J. Richardson, "All-optical phase and amplitude regenerator for next-generation telecommunications systems," Nat. Photonics **4**(10), 690–695 (2010).
4. J. Schröder, T. D. Vo, and B. J. Eggleton, "Repetition-rate-selective, wavelength-tunable mode-locked laser at up to 640 GHz." Opt. Lett. **34**, 3902-3904 (2009).
5. B. J. Eggleton, T.D. Vo, R. Pant, J. Schröder, M. D. Pelusi, D. Yong Choi, S. Madden, and B. Luther-Davies, "Photonic chip based ultrafast optical processing based on high nonlinearity dispersion engineered chalcogenide waveguides," Laser Photonics Rev. **6**(1), 97–114 (2012).
6. C. M. Caves, "Quantum limits on noise in linear amplifiers," Phys. Rev. D Part. Fields **26**(8), 1817–1839 (1982).
7. The LIGO Scientific Collaboration, "A gravitational wave observatory operating beyond the quantum shot-noise limit," Nat. Phys. **7**(12), 962–965 (2011).
8. C. J. McKinstrie, J. D. Harvey, S. Radic, and M. G. Raymer, "Translation of quantum states by four-wave mixing in fibers," Opt. Express **13**(22), 9131–9142 (2005).
9. H. J. McGuinness, M. G. Raymer, C. J. McKinstrie, and S. Radic, "Quantum frequency translation of single-photon states in photonic crystal fiber," Phys. Rev. Lett. **105**(9), 093604 (2010).
10. J. Kakande, A. Bogris, R. Slavik, F. Parmigiani, D. Syvridis, P. Petropoulos, and D. J. Richardson,"First demonstration of all-optical QPSK signal regeneration in a novel multi-format phase sensitive amplifier," in European Conference on Optical Communication ECOC, (Turin, 2010), paper PDP 3.3.

#184512 - $15.00 USD Received 30 Jan 2013; revised 16 Mar 2013; accepted 17 Mar 2013; published 25 Mar 2013

11. K. Croussore and G. Li, "Phase regeneration of NRZ-DPSK signals based on symmetric-pump phase-sensitive amplification," IEEE Photon. Technol. Lett. **19**(11), 864–866 (2007).
12. T. Torounidis and P. Andrekson, "Broadband single-pumped fiber-optic parametric amplifiers," IEEE Photon. Technol. Lett. **19**(9), 650–652 (2007).
13. J. Kakande, R. Slavik, F. Parmigiani, A. Bogris, D. Syvridis, L. Grüner-Nielsen, R.P. Petropoulos and D. J. Richardson, "Multilevel quantization of optical phase in a novel coherent parametric mixer architecture," Nat. Photonics **5**(12), 748–752 (2011).
14. K. J. Lee, F. Parmigiani, S. Liu, J. Kakande, P. Petropoulos, K. Gallo, and D. J. Richardson, "Phase sensitive amplification based on quadratic cascading in a periodically poled lithium niobate waveguide," Opt. Express **17**(22), 20393–20400 (2009).
15. B. J. Puttnam, D. Mazroa, S. Shinada, and N. Wada, "Phase-squeezing properties of non-degenerate PSAs using PPLN waveguides," Opt. Express **19**(26), B131–B139 (2011).
16. A. Szabo, B. J. Puttnam, D. Mazroa, S. Shinada, and N. Wada, "Investigation of an all-optical black-box PPLN-PPLN BPSK phase regenerator," IEEE Photon. Technol. Lett. **24**(22), 2087–2089 (2012).
17. U. Takeshi, H. Takenouchi, and M. Asobe, "First demonstration of in-line phase sensitive amplifier based on PPLN waveguide," in ECOC (Amsterdam, 2012), conference paper Tu.3.E.1.
18. J. Leuthold, C. Koos, and W. Freude, "Nonlinear silicon photonics," Nat. Photonics **4**(8), 535–544 (2010).
19. B. Eggleton, B. Luther-Davies, and K. Richardson, "Chalcogenide photonics," Nat. Photonics **5**(3), 141–148 (2011).
20. M. R. E. Lamont, C. M. de Sterke, and B. Eggleton, "Dispersion engineering of highly nonlinear As_2S_3 waveguides for parametric gain and wavelength conversion," Opt. Express **15**(15), 9458–9463 (2007).
21. C. J. McKinstrie and S. Radic, "Phase-sensitive amplification in a fiber," Opt. Express **12**(20), 4973–4979 (2004).
22. J. Fan and A. Migdall, "Phase-sensitive four-wave mixing and Raman suppression in a microstructure fiber with dual laser pumps," Opt. Lett. **31**(18), 2771–2773 (2006).
23. K. A. Croussore and G. Li, "Phase regeneration of DPSK signals based on symmetric-pump phase-sensitive amplification in bismuth oxide highly nonlinear fiber," in Conference on Lasers and Electro-Optics CLEO, (2007), paper CMZ4.
24. M. A. Ettabib, F. Parmigiani, X. Feng, L. Jones, J. Kakande, R. Slavik, F. Poletti, G. M. Ponzo, J. Shi, M. N. Petrovich, W. H. Loh, P. Petropoulos, and D. J. Richardson,"Phase regeneration of DPSK signals in a highly nonlinear lead-silicate W-type fiber," Opt. Express **20**(24), 27419–27424 (2012).
25. P. Frascella, S. Sygletos, F. C. Garcia Gunning, R. Weerasuriya, L. Grüner-Nielson, R. Phelan, J. O'Gorman, and A. D. Ellis,"DPSK signal regeneration with a dual-pump nondegenerate phase-sensitive amplifier," IEEE Photon. Technol. Lett. **23**(8), 516–518(2011).
26. R. Tang, J. Lasri, P. S. Devgan, V. Grigoryan, P. Kumar, and M. Vasilyev, "Gain characteristics of a frequency nondegenerate phase-sensitive fiber-optic parametric amplifier with phase self-stabilized input," Opt. Express **13**(26), 10483–10493(2005).
27. J. Kakande, C. Lundström, P. A. Andrekson, Z. Tong, M. Karlsson, P. Petropoulos, F. Parmigiani, and D. J. Richardson, "Detailed characterization of a fiber-optic parametric amplifier in phase-sensitive and phase-insensitive operation," Opt. Express **18**(5), 4130–4137(2010).
28. M. A. F. Roelens, S. Frisken, J. A. Bolger, D. Abakoumov, G. Baxter, S. Poole, and B. J. Eggleton, "Dispersion Trimming in a reconfigurable wavelength selective switch," J. Lightwave Technol. **26**(1), 73–78 (2008).
29. M. Gao, T. Inoue, T. Kuroso, and S. Namiki, "Evolution of the gain extinction ratio in dual-pump phase sensitive amplification," Opt. Lett. **37**(9), 1439–1441 (2012).
30. T. D. Vo, R. Pant, M. D. Pelusi, J. Schröder, D. Choi, S. K. Debbarma, S. J. Madden, B. Luther-Davies, and B. J. Eggleton, "Photonic chip-based all-optical XOR gate for 40 and 160 Gbit/s DPSK signals," Opt. Lett. **36**(5), 710–712 (2011).
31. N. K. Langford, S. Ramelow, R. Prevedel, W. J. Munro, G. J. Milburn and A. Zeilinger, "Efficient quantum computing using coherent photon conversion," Nature **478**(7369), 360–363 (2011).

1. Introduction

Nonlinear optical parametric processes have received much research attention for their potential in applications such as the implementation of phase-sensitive optical parametric amplifiers (OPAs) [1–3], the mode-locking of lasers [4] or all-optical signal processing [5].

The potential for noiseless amplification and generation of non-classical squeezed states of light [6] due to the ability of phase-sensitive amplifiers (PSAs) to amplify or attenuate quadratures of an electric field has lead to their application to diverse tasks including the laser interferometer gravitational wave observatory (LIGO) [7] or quantum state translation by Bragg scattering [8, 9]. For optical telecommunication applications optical PSAs are particularly attractive

#184512 - $15.00 USD Received 30 Jan 2013; revised 16 Mar 2013; accepted 17 Mar 2013; published 25 Mar 2013

due to their potential to realize regeneration of phase-encoded signals [3, 10, 11], with bandwidths similar to phase-insensitive OPAs [12]. Phase regeneration of both Differential Phase Shift Keying (DPSK) and Quadrature Phase Shift Keying (QPSK) signals have been demonstrated using these devices with the potential for generalization to higher orders of PSK phase regeneration [10, 13].

Photonic integration, i.e. the miniaturization and combination of several optical functionalities and components into a single platforms promises a significant simplification of the manufacturing of photonic devices similar to electronic integrated circuits. Simultaneously this reduction in scale would benefit the implementation of optical PSAs for signal processing by reducing walk-off and the effect of phase-mismatch.

To realize this photonic integration, the elements mediating nonlinear interactions, such as the nonlinear fibers used in current generation phase-sensitive OPAs, must be significantly scaled down in size. The first demonstrations of On-chip phase-sensitive parametric amplifiers were based on the second-order susceptibility tensor $\chi^{(2)}$ in periodically poled Lithium Niobate (PPLN) waveguides [14]. Phase regeneration of a 10 Gb/s binary phase shift keying (BPSK) [15, 16] and 40 Gb/s DPSK [17] signal were demonstrated. However, so far all demonstrations of phase sensitive amplification using four-wave mixing based on the third-order Kerr-nonlinearity ($\chi^{(3)}$) were performed in optical fibers. Chip-based $\chi^{(3)}$ devices could offer an alternative capable of higher bandwidth operation without strict temperature control and the potential for easier integration with other processing functionalities.

In the context of investigating chip-based $\chi^{(3)}$ nonlinear devices for photonic integration, silicon and chalcogenide glass have both generated significant interest due to their high intrinsic $\chi^{(3)}$ nonlinearity [18, 19]. The strong nonlinear response of these materials and the tight confinement of the fundamental mode, (resulting in a $\gamma \sim 100$ to 1000 times that of highly nonlinear silica fiber) enables waveguides on the scale of centimetres or even millimetres, rather than metres, with comparable nonlinearity to current highly-nonlinear fibers. Dispersion engineering these centimetre scale waveguides promises improved broadband operation compared to fibre-based PSAs [5, 20]. While silicon has the advantage that it is compatible with established CMOS fabrication techniques, it is hindered by two-photon absorption (TPA) and the generation of free carriers which limit the maximum achievable nonlinear phase shift [18]. In comparison, chalcogenide glass (As_2S_3) has very low TPA and lacks free carriers, greatly simplifying the dynamics of nonlinear processes [19].

There are two main architectures for providing phase-sensitive amplification in $\chi^{(3)}$ materials [21]; signal-degenerate [3, 10, 11, 22–25] and pump-degenerate [1, 2, 26, 27] FWM. In this paper we use the former to demonstrate $\chi^{(3)}$ phase-sensitive amplification of light in a photonic chip based on a dispersion-engineered chalcogenide ridge waveguide. Our experimental setup is based on a spectral pulse shaping scheme which generates signal, idler and pump via spectral slicing from a single broadband pulse source. This method automatically generates synchronization between all waves while enabling tight control over their relative phases, providing an elegant experimental system for the investigation of PSAs on novel platforms. It further enables us to avoid the use of continuous wave pumps whose high average powers are beyond damage thresholds of current state-of-the-art chalcogenide waveguides. The maximum extinction of the phase-sensitive gain observed was 9.9 dB.

2. Principle and experiment

Figure 1 illustrates the two main FWM schemes to implemente $\chi^{(3)}$ phase-sensitive amplification. In order to observe the phase-sensitive nature of the gain, all four waves in the FWM interaction must be seeded. The schemes differ in their degeneracy of the waves, i.e. which waves in the interaction are degenerate. In the signal-degenerate architecture [Fig. 1(a)] a de-

#184512 - $15.00 USD Received 30 Jan 2013; revised 16 Mar 2013; accepted 17 Mar 2013; published 25 Mar 2013

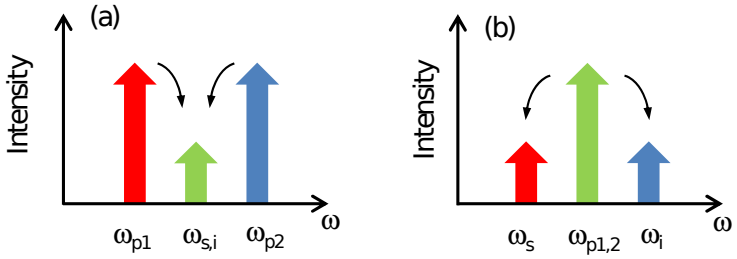

Fig. 1. (a) Signal-degenerate phase-sensitive FWM. $\omega_{p1,2}$ and $\omega_{s,i}$ are the pump and degenerate signal/idler frequencies. (b) Pump-degenerate phase-sensitive FWM scheme. ω_s, ω_i and ω_p are the signal, idler and degenerate pump frequencies. Solid black arrows denote direction of energy transfer during FWM.

generate signal/idler wave at ω_s is centered between two strong pump waves at frequencies ω_{p1} and ω_{p2} [21]. The signal and idler waves represent a data signal input to a practical phase-sensitive amplifier. For the second, pump-degenerate architecture, the signal and idler waves at separate frequencies (ω_s, ω_i) copropagate with two frequency degenerate pumps waves (ω_p). The signal and idler waves are amplified by phase-sensitive FWM as they propagate through the nonlinear waveguide. We label this the pump-degenerate phase-sensitive four-wave mixing scheme [Fig. 1(b)]. Here we chose to implement the PSA using the signal-degenerate scheme, as it offers advantages for implementing a practical PSA for actual telecommunication signals as both signal and idler are located at the same wavelength.

To observe the phase-sensitive gain it is necessary to generate a set of synchronized pulsed signal, idler and pump waves with a constant relative phase relation. To observe the variation in signal power as a function of phase, i.e. the phase-sensitive gain, the relative phase between all waves is then controlled by applying a phase-shift $(\Delta\phi)$ to one or more of the initial waves. All waves are then coupled into a chalcogenide chip in which the FWM occurs. The resulting output spectrum is detected and as the relative phase is varied, the power of the signal as a function of phase is measured.

Figure 2 depicts the experimental setup. We generate the synchronized pulses by slicing the pump, signal and idler waves from a single high power MLL source with ∼30 nm bandwidth. Figure 3 depicts the initial spectrum of the laser [Fig. 3(a)] and the spectrally sliced output comprising the degenerate signal and the two pump waves [Fig. 3(b)]. The resulting pulses are copolarized, synchronized in time and have identical repetition rates. By slicing all the waves from a single pulse source, the resulting waves are also automatically phase-locked. A similar approach was used in [22], in which a pair of phase coherent pumps were derived from a quasi-supercontinuum source. Rather than using a system of gratings and lenses as in [22], a spectral pulse shaper (SPS 1, Finisar Waveshaper) [28] was used as a programmable filter to spectrally slice the MLL source. Due to the pulsed nature of the waves, stimulated Brilloin scattering (SBS) can be avoided and does not play a role in this experiment.

The total average power at the output of SPS 1 was approximately -10 dBm. The pumps and degenerate signal/idler waves were reamplified by a short pulse Erbium-doped fiber amplifier (EDFA) to an average power of 13 dBm. A second Waveshaper (SPS 2) was then used to either block or pass the pump waves to control the FWM interaction as well as to filter out amplified spontaneous emission (ASE) noise introduced in the previous stage. Additionally, SPS 2 was used to control the overall phase-relation of all waves by applying phase-shifts $(\Delta\phi)$ to the center wave (see spectra in Fig. 2). The polarization of all waves was then aligned to the TM mode of the chalcogenide waveguide and coupled to the chip via lens-tipped fibers. The coupling loss at each fibre facet was ∼4 dB. At the output of the waveguide, the spectrum was

#184512 - $15.00 USD Received 30 Jan 2013; revised 16 Mar 2013; accepted 17 Mar 2013; published 25 Mar 2013

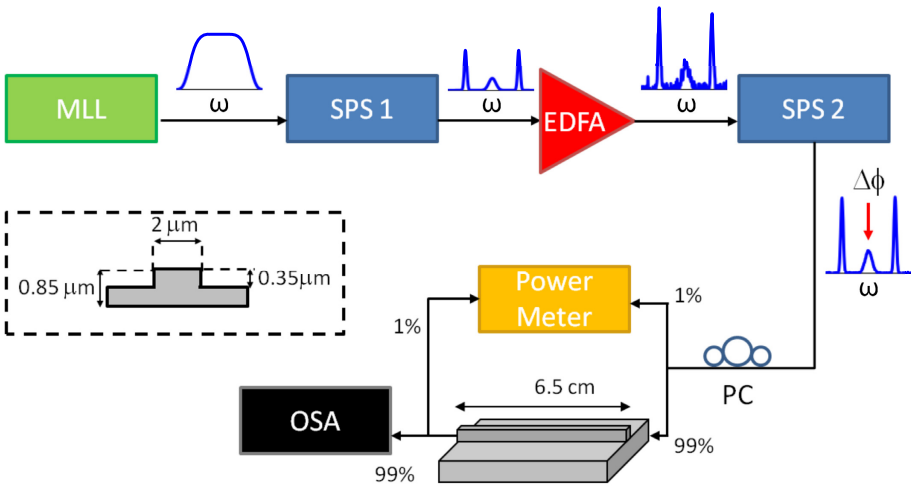

Fig. 2. MLL = mode locked laser, SPS = spectral pulse shaper, EDFA = erbium doped fibre amplifier, PC = polarization controller, OSA = optical spectrum analyzer. The mode locked laser (MLL) is a 38.6 MHz fibre laser which generates 300 fs pulses with 160 W peak power. The output is spectrally sliced into three waves at SPS 1 and amplified in an EDFA. A second SPS tunes the phase ($\Delta\phi$) of the central signal. The polarization of all three waves is aligned to the TM waveguide mode and coupled onto the chip. A power meter monitors the input and output power to the chip. The output spectrum is detected on an OSA. The blue traces are schematics of the spectrum at each point in the experiment. The inset shows a cross-section of the chalcogenide waveguide with the associated dimensions.

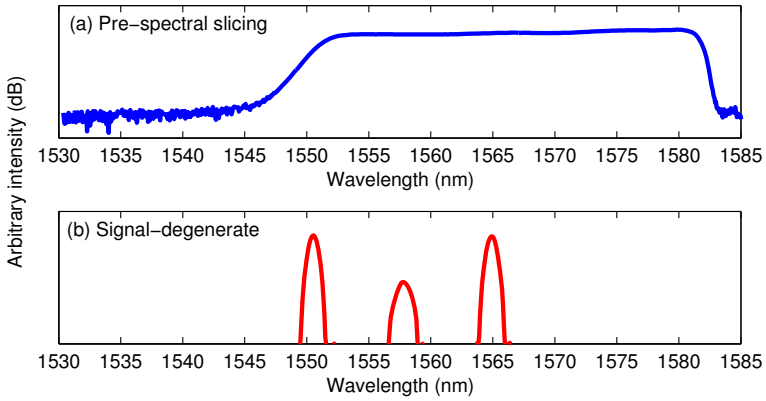

Fig. 3. Typical normalized spectrum at (a) the output of the mode locked laser and at (b) the output of SPS 2 after spectral slicing (lower) for signal-degenerate FWM.

detected on an optical spectrum analyzer (OSA). As the relative phase was varied at SPS 2, the on-chip signal gain was calculated by taking the ratio of the spectral power of the amplified signal after the chip to the unamplified signal after the chip, when the pump waves were blocked by SPS 2.

The nonlinear medium was a 6.5 cm ridge waveguide (see inset in Fig. 2) fabricated from chalcogenide (As_2S_3) glass. The transverse dimensions were 2 μm $\times$ 0.85 μm, corresponding to a total nonlinearity of γ = 9.9 $W^{-1}m^{-1}$ at 1550 nm. From calculations of the dispersion

#184512 - $15.00 USD Received 30 Jan 2013; revised 16 Mar 2013; accepted 17 Mar 2013; published 25 Mar 2013

engineering of the TM mode, we estimate the following dispersion parameters at 1550 nm: β_2 = -0.04 ps^2/m, β_3 =1.18 $\times$ 10^{-3} ps^3/m and β_4 = 8.76 $\times$ 10^{-7} ps^4/m. The zero dispersion wavelength, propagation loss and effective waveguide length associated with this mode is $\sim$1500 nm, $\alpha = 0.5$ dB/cm and 4.5 cm respectively.

The signal/idler and pump waves were generated by spectrally slicing using SPS 1. The signal/idler wave was created with a 0.13 THz Gaussian filter centered at 1557.7 nm, while the two pump waves were obtained by two 0.07 THz Gaussian filters centered at 1550.1 and 1564.5 nm. The spectral widths were chosen to achieve pulse widths on the order of 2-10 ps which were found optimal for achieving a high peak-to-average power ratio with sufficient separation between the three waves. The pumps were created spectrally narrower than the signal/idler wave so that they were were temporally broader. This minimized gain variation accros the signal pulse caused by the instantaneous intensity variation of the pumps, thus maximizing the on-chip amplification of the signal.

The power of the individual waves was controlled by attenuation in SPS 2 to maximize signal amplification. Gaussian filters identical to those used at SPS 1 were applied to the pump and signal waves to filter excess ASE noise. The temporal FWHM of the resulting pump and signal pulses was 7 ps and 4 ps respectively, as measured with an optical autocorrelator and a frequency resolved optical gating device (FROG). A constant spectral phase was varied across the signal from 0 to 2π in increments of 0.1π. On-chip, the average and peak powers of pump 1 (1550.1 nm) was 6 dBm and 4.8 W respectively. Pump 2 (1564.5 nm) was measured as 3 dBm average power and 2. 5 W peak power, while the average power of the signal/idler wave (1557.5 nm) was -22 dBm corresponding to 4 mW peak power.

3. Results and discussion

Figure 4(a) presents the amplified (solid, coloured) and unamplified signal (dotted, black) spectra measured at the output of the chip for different phases applied to the signal. The amplified signal was measured with all waves co-propagating through the waveguide, while we measured the unamplified signal when the pumps were blocked by SPS 2 and the signal was thus propagating through the chip by itself. We can clearly see the amplification experienced by the signal varies as a function of phase. The structure on the two pump waves can be attributed to SPM and XPM.

Not shown in these spectra are additional FWM products outside of the two pump waves, similar to those observed in [29]. These additional FWM products can be attributed to a combination of phase-sensitive and phase-insensitive FWM processes between the original pump and signal waves and improve the phase sensitive extinction [29]. Phase matching of these processes is a side effect of the low dispersion of the dispersion-engineered waveguide. The residual peak located at 1552.5 nm in the spectrum of the unamplified signal is because of imperfect attenuation of the pump by SPS 2, however due to its low power it is safe to assume that it does not influence the signal propagation.

The phase-sensitive signal gain was extracted from the measured spectra by integrating the spectral power of the signal over a bandwidth of 3 nm and taking the ratio to the unamplified signal power extracted in the same way. The relatively large bandwidth was chosen to ensure that we integrated over the full signal bandwidth and that the results where not affected by cross-phase modulation (XPM). We observe a sinusoidal variation in the gain as a function of phase, with a periodicity of π. Minima in the gain curve occur at 0.6π and 1.6π (-2.5 dB attenuation, see Fig. 4(c)). A maximum on-chip gain of about 8 dB is observed at detunings of 0, π and 2π radians. The phase-sensitive extinction (PSE) is defined as the difference between the maximum and minimum signal gain. By averaging over the multiple maxima and minima in Fig. 4, we obtained an on-chip PSE of 9.9 dB. The experimental results show good agreement

#184512 - $15.00 USD Received 30 Jan 2013; revised 16 Mar 2013; accepted 17 Mar 2013; published 25 Mar 2013

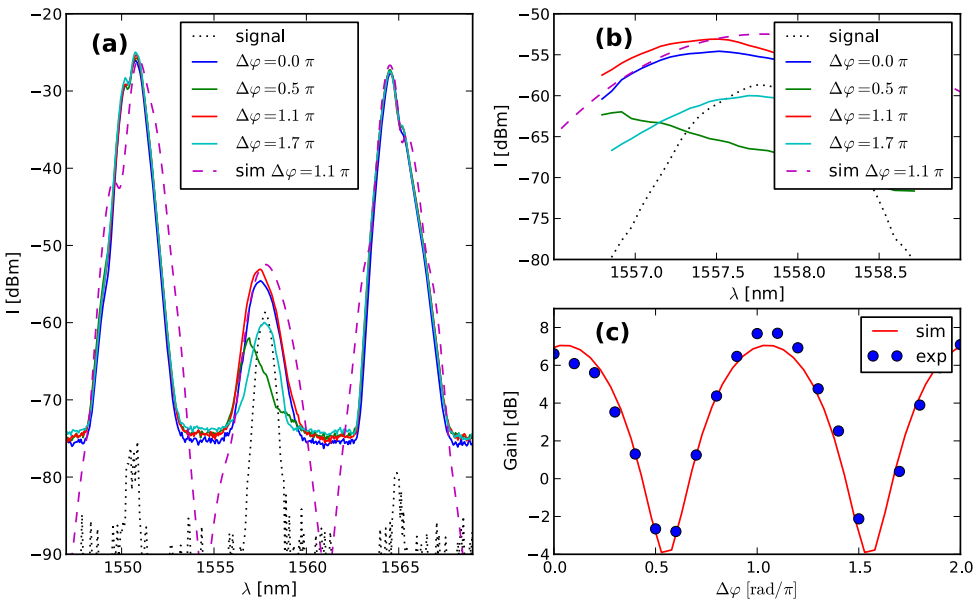

Fig. 4. (a) Unamplified signal spectrum (black dotted line) and amplified spectra (solid coloured lines) for various relative phase shifts, with a simulated spectrum for comparison (dashed line) (b) Close-up of the signal spectrum. (c) On-chip signal gain (dB) as a function of relative signal phase ($\Delta\phi$); (blue dots) experimental data, (red line) numerical simulation.

with numerical simulations of the nonlinear Schrödinger equation (NLSE) for the system with up to fourth-order dispersion using a split step Fourier method (SSFM) [Fig. 4(c) red line].

The parameters used in the simulation of the signal-degenerate FWM experiment are given in Table 1. It was necessary to slightly adjust the numerical parameters to most accurately model the experimental system. The discrepancy could be attributed to a small residual detuning between the two pump waves of about 6 ps, or similarly reduced peak powers because of errors in their estimation from the measured average powers, most likely due to ASE noise. Furthermore there is a significant uncertainty in the dispersion parameters of the waveguide, as it is inherently difficult to measure such low dispersion. In the simulation given in Fig. 4(c) we chose to use a temporal detuning between the two pumps.

Table 1. List of simulation parameters for the signal-degenerate FWM experiment. This set of parameters was used to generate the simulation data in Fig. 4 (e).

β_2	-0.04 ps^2m^{-1}	P_{signal}	4 mW
β_3	0.001176 ps^3m^{-1}	$FWHM_{pump1,2}$	0.07 THz
β_4	8.76×10^{-7} ps^4m^{-1}	$FWHM_{signal,idler}$	0.13 THz
P_{pump1}	4.8 W	γ	9.9 $W^{-1}m^{-1}$
P_{pump2}	2.5 W		

We observed 10 dB of on-chip PSE. Compared to other values reported in the literature (20 dB reported by Slavik et. al. [3]) this is relatively low. Even more so, as our effective nonlinear phase shift derived from simulations (0.5π, 0.8π) was comparable to that used in [3] (0.6π). This difference in extinction most probably has a number of reasons. Firstly, in contrast to [3],

#184512 - $15.00 USD Received 30 Jan 2013; revised 16 Mar 2013; accepted 17 Mar 2013; published 25 Mar 2013

we use pulsed signal, pump and idler waves. thus the parametric gain across the signal/idler is not uniform, although we tried to minimize this effect by using temporally longer pump pulses. Furthermore, variation in the instantaneous intensity results in a complicated evolution of the SPM and XPM induced nonlinear phase shift which in turn affects the phase-matching condition over the length of the waveguide.

The PSE achieved in our experiments is still sufficient however, to perform phase-regeneration of phase modulated signals. A $\chi^{(2)}$-based PSA with 6 dB of PSE was shown to provide regeneration of a 10 Gb s^{-1} BPSK modulated signal [15]. FWM-based PSAs with similar values of PSE (12 dB and 4.4 dB) have also been implemented in the phase-regeneration of DPSK signals [23, 24]. With the PSE reported here, these results indicate that using current chalcogenide chips, we are already capable of generating a sufficient level of PSE for on-chip phase regeneration. In a broader context, the results presented in this paper also indicate that chalcogenide glass chips are capable of handling the presence of multiple pulses necessary for FWM [30]. This suggests that these photonic chips can potentially support the FWM Bragg scattering effect and the dispersion engineering required to demonstrate quantum state translation [8,9] as well as coherent photon conversion [31] which can lead to efficient optical quantum computation and communication.

While power handling and residual phase-mismatch and propagation loss pose a significant hurdle for achieving sufficient PSE using continuous wave (cw) pumping in the current generation of chalcogenide waveguides, we are confident that these can be overcome through shifting the zero-dispersion wavelength further to 1550 nm and improvements in propagation and coupling loss for next generation waveguides. Although there are still improvements to be made in terms of the material properties of available chalcogenide chips, this work was a successful proof of principle demonstration of phase-sensitive amplification in a chalcogenide chip.

4. Conclusion

We demonstrated approximately 10 dB extinction of phase-sensitive on-chip gain via dual-pump FWM inside a chalcogenide waveguide. This is to the best of our knowledge the first demonstration of phase-sensitive amplification in a $\chi^{(3)}$ nonlinear photonic chip. This proof of concept experiment is the first step towards the photonic integration of phase-sensitive amplifiers for potential phase regeneration of data signals, and demonstrates the feasibility of high-power parametric processes in current chalcogenide ridge waveguides.

Acknowledgments

This work was supported by the Australian Research Councils (ARC), Federation Fellowship (FF0776056), Centre of Excellence CUDOS (CE110001018), Laureate Fellowship (FL120100029) and Discovery Early Career Researcher (DE120101329) schemes.

#184512 - $15.00 USD Received 30 Jan 2013; revised 16 Mar 2013; accepted 17 Mar 2013; published 25 Mar 2013